Research Paper

HIGH-ENERGY RADIATION EFFECTS ON SILICON NPN BIPOLAR TRANSISTOR ELECTRICAL PERFORMANCE: A STUDY WITH 1 MEVPROTON IRRADIATION

Godwin Jacob D' Souza
Associate Professor, Dept. of Electronics,
St Joseph's College (Autonomous) Bangalore.

ABSTRACT:

This study explores the degradation of the silicon NPN transistor's emitter-base junction, specifically focusing on the 2N2219A model, when subjected to both forward and reverse polarization. The research investigates the current-voltage characteristics affected by 1 MeV proton irradiation at different fluencies: 5.3×10^{8}, 5.3×10^{10}, 5×10^{11}, 5×10^{12}, and 5×10^{13} protons/cm^2, all conducted at 307 K. The experimental results reveal a significant correlation between diode parameters—such as reverse saturation current, series resistance, and non-ideal factor—and the intensity of proton exposure. This correlation underscores that the degradation induced by protons primarily stems from displacement damage. The observed degradation is predominantly attributed to the creation of defects and interfacial traps within the transistor due to exposure to high-energy radiation. The findings suggest that the effects of irradiation align more closely with the compensation phenomenon in doping rather than its enhancement.

KEYWORDS: silicon transistors; NPN-BJTs; emitter-base; proton irradiation; electric performance.

1. INTRODUCTION

In the contemporary world, where nuclear technology, satellites, and aeronautics play increasingly crucial roles, there is a rising demand for semiconductor devices capable of enduring radiation-intensive environments. This demand has spurred extensive research efforts aimed at meeting this critical need.

Among semiconductor devices, silicon-based bipolar junction transistors (BJTs) have emerged as leading candidates for such applications, owing to their versatile utility across a wide range of electronic circuits [1–3]. Significant attention is directed towards examining the emitter-base junction of silicon NPN transistors, given their essential role as integral components in modern electronics [4,5].

Understanding the behavior of silicon-based BJTs, especially their emitter-base junction, in irradiation conditions is crucial. BJTs are essential for signal amplification, switching, and various electronic systems. Their reliable performance in radiation-rich environments is vital for nuclear technology, satellites, aeronautics, and other critical applications.

For instance, radiation can significantly affect FET-based devices, causing changes in electrical characteristics, performance degradation, and the introduction of defects or traps within the device, thereby impacting its functionality and reliability [6–8]. This study offers an opportunity to innovate radiation monitoring devices, such as radiation-sensitive metal-oxide-silicon field-effect transistors (RADFETs) and dosimeter devices based on PNP structures. RADFETs have proven effective in space missions and laboratories for measuring radiation doses. They generate continuous electrical outputs, which are electronically converted to

accurately assess accumulated doses. This remote monitoring and display capability makes them highly versatile [9].

To ensure the reliability and functionality of these electronic components under challenging conditions, it has become essential to study the effects of irradiation on their electrical performance. Effective investigations require comprehensive studies using particles capable of inducing defects in semiconductor materials. Protons are particularly advantageous due to their ability to generate defects at a significantly higher rate compared to other particles like neutrons and electrons [10].

Numerous studies have explored irradiation-induced damage and developed effective procedures for radiation hardening of metal-oxide-silicon (MOS) and bipolar silicon (Si) devices, facilitating their seamless integration [11–15]. For example, Ohyama et al. examined the degradation in electrical characteristics of both n + p and p + n silicon junctions under the influence of 1 MeV neutron and 1–2 MeV electron irradiation [16]. Hefner et al. investigated the effects of neutrons on insulated gate bipolar transistors (IGBTs) [17]. Omotoso et al. studied the impact of high-energy electron irradiation on the Schottky barrier height and the Richardson constant of Ni/4H-SiC Schottky diodes [18].

Recently, Pearton et al. demonstrated the effects of ionizing radiation damage on GaN devices [19]. They showed that proton and electron irradiation in HEMTs results in positive threshold voltage shifts due to electron trapping at defects, which reduces carrier mobility and degrades drain current and trans conductance [20]. Schwarz et al. investigated the impact of gamma irradiation on electronic carrier transport in AlGaN/GaN high electron mobility transistors (HEMTs) [21].

Previous studies have also highlighted the degradation of electrical properties in silicon junctions under irradiation. In our own research, we observed significant changes in the optical properties of silicon junctions when exposed to irradiation. Specifically, under forward bias conditions and an irradiation fluence of 5 × 10^12 protons/cm^2, we noted a drastic reduction in electroluminescence intensity by up to 96% [22–24].

Building upon this groundwork, our study aims to comprehensively investigate the effects of 1 MeV proton irradiation on the electrical characteristics of silicon emitter-base bipolar junction transistors (BJTs). Our focus will be on the emitter-base junction within commercially available 2N2219A silicon NPN transistors by ST Microelectronics.

2. Experimental Setup and Materials

For this study, we selected silicon NPN bipolar emitter-base transistors of the 2N2219A model, manufactured by ST Microelectronics in Geneva, Switzerland, as our test samples. These transistors have fixed emitter and base areas measuring 0.01 mm^2. The sample preparation involved metallizing the top surface of the transistors with a uniform 1.6 µm layer of aluminum, while the top face was passivated with SiO2 and the back face was coated with 0.3 µm of gold. Figure 1 illustrates the commercial 2N2219A NPN transistor used in this investigation.

The 2N2219A transistor is a silicon Planar Epitaxial NPN transistor housed in a metal body, adhering to the Jedec TO-39 standard (2N2219A) and the TO-18 standard (2N2222A) [25]. It is specifically designed for high-speed switching applications and can handle collector currents up to 500 mA. Additionally, it offers excellent current gain across a wide range of collector currents, minimal leakage currents, and low saturation voltage. Detailed technical specifications for the 2N2219A NPN transistor can be found on the STMicroelectronics website [25].

Figure 1. The official design of the commercialized 2N2219-NPN transistor by STMicroelectronicsInc. features the schematic electronic symbol. Adapted from [25].

The primary focus of this investigation was on studying the behavior of the emitter-base (E-B) junction, while leaving the collector terminal floating. Current-voltage (I-V) characteristics were characterized using a parametric analyzer controlled by a computer via an IEEE bus interface. Irradiation experiments were conducted using a Faraday cup designed for precise measurement of proton fluences.

To ensure strict control over experimental conditions, a proton beam source was used, with the current maintained below 3 nA. Various parameters including proton beam flux and energy, irradiation temperature set at 307 K, and controlled elapsed time between irradiation and measurement were rigorously monitored.

Current-voltage measurements were taken precisely 5 minutes after irradiation cessation to evaluate immediate proton-induced effects. Measurement accuracy was maintained with a standard deviation of 3% using a total of 15 diodes in the experimental setup.

All experiments were conducted at the electrical engineering and nuclear laboratories located within the physics departments of Sherbrooke and Montreal universities in Canada.

3. RESULTS AND DISCUSSION

To analyze the current-voltage characteristics of our specimens, we begin by identifying the constituent current components that contribute to the overall junction current. Under forward bias conditions, two main components are considered: the bulk diffusion current, which originates from the neutral region, and the bulk generation-recombination current, occurring within the depletion region. The resistivity of the distinct regions of the junction—emitter, base, and ohmic contact—further influences the total current, which can be expressed as follows [26]:

$$I = I_s \left[\exp\left(\frac{q(V-R_s I)}{nk_B T}\right)\right] - 1, \quad (1)$$

where R_s is the series resistance, I_s is the reverse saturation current, n is the non-ideality factor, q is the electron charge, T is the absolute temperature, and k_B is the Boltzmann's constant. The measure of n depends on which current component is dominated in a specific operating regime.

For reverse bias conditions, the main contribution to the junction current arises from generation-recombination processes involving deep centers. In our model, we do not consider the tunneling component. This current is influenced by both temperature and the applied voltage, and can be described by the following expression [26]:

$$I_R \propto \sqrt{T}\sqrt{V_{Rexp}}\left(-\frac{E_\alpha}{k_B T}\right)\exp(CV_R), \quad (2)$$

Figure 2 provides a comprehensive overview of the changes in the current-voltage (I-V) characteristics of silicon-based NPN (emitter-base) junctions under forward bias conditions, considering the influence of irradiation at an operating temperature of 307 K. A notable observation in these characteristics is the noticeable increase in the threshold voltage with increasing irradiation fluence. This trend is particularly significant as it indicates that the junction becomes less favorable for forward bias operation as it experiences higher levels of irradiation.

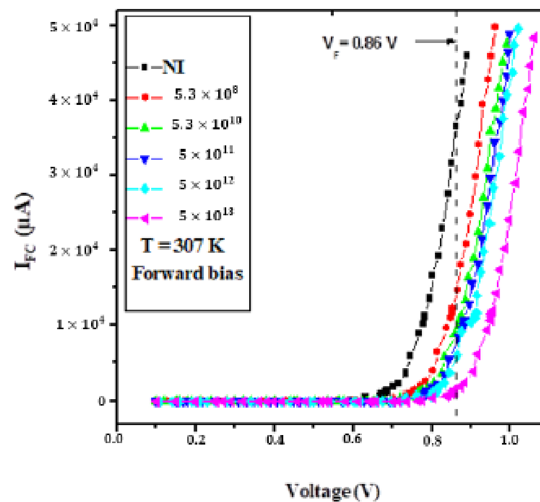

Figure 2. The forward bias I–V characteristics of bulk silicon (NPN) emitter-base at 307 K are presented, incorporating the impact of 1 MeV proton irradiation.

Furthermore, when a constant voltage is applied across the NPN junction, the current exhibits a consistent and significant decrease with increasing irradiation fluences. This observed reduction in current flow due to irradiation has profound implications for the performance and behavior of silicon-based NPN junctions, especially under forward bias conditions.

The introduction of defects and traps into the silicon material, induced by irradiation, fundamentally alters the semiconductor's conductivity through several mechanisms. First, these defects act as barriers or recombination sites for charge carriers, hindering their free movement within the crystal lattice. This increased trapping and recombination disrupt the smooth flow of charge carriers, thereby reducing the overall current. Second, the traps create energy levels within the semiconductor bandgap, influencing charge carrier behavior. These energy levels can capture and release charge carriers at different rates, affecting carrier mobility and recombination processes.

As a result, the findings presented in Figure 2 underscore the critical role of irradiation in shaping the performance of silicon-based NPN junctions. These insights are particularly significant for applications in radiation-sensitive environments and electronics. Understanding

the profound impact of irradiation on device characteristics is crucial for fields where radiation tolerance and reliability are paramount, such as aerospace, nuclear technology, and medical equipment.

By comprehensively understanding the complex interaction between irradiation and semiconductor behavior, engineers and researchers can design and optimize devices capable of withstanding or even leveraging irradiation in various practical applications. This ensures the integrity and functionality of electronic systems in challenging and radiation-rich environments.

Figure 3 explores the profound impact of irradiation on the current-voltage (I-V) characteristics of a semiconductor device, cleverly depicted on a semi-logarithmic (semilog) scale at an operating temperature of 307 K. The semilog representation provides a unique viewpoint that accentuates subtle details in the I-V curve, which may not be as discernible on a linear scale. This representation serves as a powerful tool for analyzing semiconductor behavior under varying conditions, such as irradiation.

One of the most notable observations in Figure 3 is the segmentation of the I-V curve into two distinct regions, each characterized by different slopes. These two segments suggest that irradiation significantly alters the semiconductor's behavior, leading to the emergence of two distinct electrical response modes. The differing slopes indicate a pronounced shift in the device's electrical characteristics and behavior.

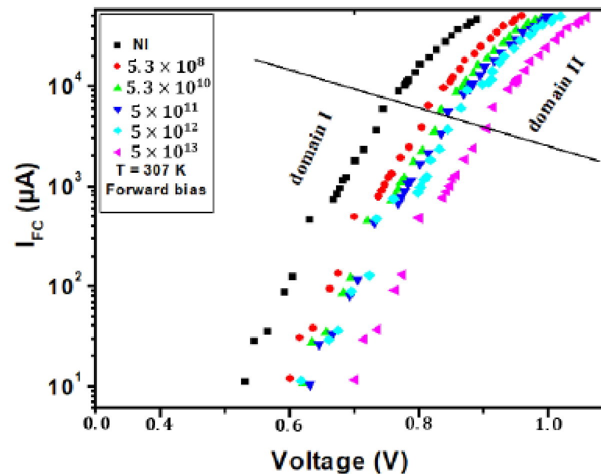

Figure 3. The semilogarithmic representation of the I–V characteristics for bulk silicon NPN emitter- base junctions under forward bias at 307 K is depicted, accounting for the influence of irradiation.

To comprehensively analyze and interpret our experimental data, we utilize Equation (1) as our foundational mathematical framework. This equation provides insights into the relationship between current (I) and voltage (V) in the context of the irradiated semiconductor device. However, the device's behavior is dynamic and varies with the level of irradiation. To account for these variations, we introduce fitting parameters—Is, n, and Rs—that are specific to each irradiation condition. These parameters allow us to adjust the equation to fit each distinct region observed in the I-V curve. By extracting and applying these fitting parameters for each irradiation condition and each of the two distinct domains, we gain a nuanced understanding of how the characteristics of the semiconductor device evolve in response to irradiation.

Furthermore, the results of the series resistance (Rs) and the non-ideality factor (n) are graphically depicted in Figure 3. A noticeable increase in Rs with higher levels of irradiation is observed. This phenomenon is attributed to the introduction of defects into the microelectronic structure, as evidenced by documented increases in resistivity within silicon diodes, as reported in previous studies [16]. Consistent with earlier findings [27], it is established that resistance linearly escalates with increasing irradiation fluences across all cases.

These insights are crucial for both understanding the fundamental physics of the device and for designing semiconductor components that can withstand or even utilize irradiation in practical applications, such as in radiation-hardened electronics or semiconductor-based radiation sensors.

To quantify the experimental damage factor, the outcomes were subjected to fitting. The damage factor is defined as the measure of degradation or alteration in the device's performance due to irradiation. It encapsulates the changes observed in electrical characteristics such as current-voltage behavior, threshold voltage, and series resistance (Rs).

Calculating the series resistance (Rs) in junctionless transistors involves considering the total resistance encountered by electric current within the device. This cumulative resistance stems from multiple sources, including the semiconductor channel, contact interfaces, and intermediate materials. It is significantly influenced by physical factors such as carrier mobility, impurities, and defects within the semiconductor material. Rs encompasses resistance at the metal-semiconductor contacts and throughout the conducting channel. Understanding Rs is crucial as it directly impacts the device's electrical behavior and overall performance.

For more comprehensive insights into this topic, please refer to the cited references [28–30].

$$R_s = R_S^0(1 + k_R \emptyset), \quad (3)$$

where R^0 and R_s are the series resistance before and after irradiation, respectively, k_R is the linear series resistance damage factor, and ∅ is the irradiation fluency.

Figure 4 depicts the investigation of the ideality factor (n) and series resistance (Rs) of the silicon NPN emitter-base junction as they change with 1 MeV proton irradiation fluence at an operating temperature of 307 K within Domain I. The findings within Domain II exhibit a close correlation with those observed in Domain I. The fitting results are graphically illustrated by the solid line.

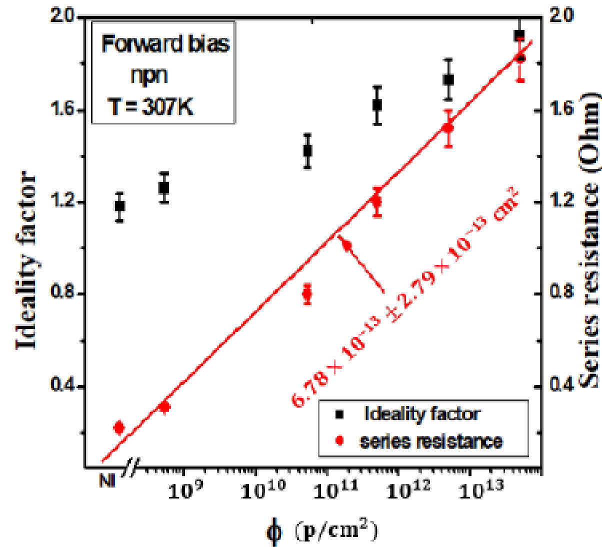

Figure 4. The ideality factor and series resistance of the silicon (npn) emitter-base junction were studied as a function of 1 MeV proton irradiation fluence at 307 K in Domain I. The results in DomainII closely matched those in Domain I. Fitting results are shown by the solid line.

Figure 4 reveals a clear trend where the saturation current significantly increases in response to irradiation. This pattern closely mirrors the dependency observed in the series resistance (Rs), indicating a direct correlation between irradiation levels and both saturation current and series resistance. The experimental data underwent fitting procedures using Equations (3) and (4), from which linear factor damage coefficients were derived: k_R =(6.87±2.79)×10^{-13} cm², k_I =(2.75±1.12)×10^{-12} cm² (Domain I), and k_I =(1.37±0.69)×10^{-12} cm² (Domain II). The observed trend highlights that the increase in the non-ideality factor (n) is more pronounced than that of the series resistance (Rs). This suggests that the defects introduced by irradiation, which elevate Rs, do not collectively contribute to the increase in n. kI represents the linear saturation current damage factor, indicating how rapidly the saturation current of the semiconductor device increases due to irradiation. In Domain I, k I is higher (2.75 ± 1.12) ×10−12×10^{-12} cm², reflecting a substantial impact on saturation current. In Domain II, k I is lower (1.37± 0.69) ×10^{-12} cm², indicating a milder response to irradiation in this domain. These values provide insights into the specific changes in saturation current in response to irradiation within each domain.

Overall, Domain I exhibits more significant changes in saturation current, series resistance, and non-ideality factor in response to irradiation compared to Domain II. This discrepancy suggests that the influence of irradiation on the electrical characteristics of the semiconductor device is more pronounced in Domain I, while Domain II shows a comparatively milder response to irradiation.

$$I_s = I_s^0(1 + k_I \emptyset), \qquad (4)$$

where I^0 and I_s are the saturation current before and after irradiation, respectively, and k_I is the linear saturation current damage factor.

Figure 5 offers detailed insight into how the reverse saturation current of a silicon NPN emitter-base junction behaves under varying levels of irradiation at an operating temperature of 307 K. These data are segregated into two distinct domains for clarity, with solid lines representing results derived from fitting procedures.

A striking observation is the consistent increase in the parameter n as irradiation levels intensify. Specifically, n rises from 1.18 ± 0.06 for unirradiated samples to 1.92 ± 0.07 when the fluence reaches 5×10^{13} cm^{-2}.

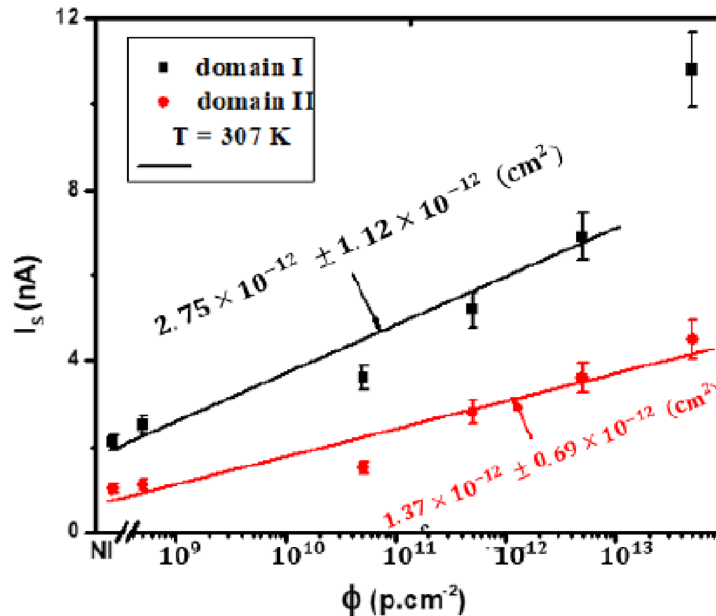

Figure 5. The reverse saturation current of the silicon NPN emitter-base junction at 307 K as a function of irradiation fluences, delineated for two distinct domains. The solid lines represent the outcomes of the fitting procedure.

This shift in *n* is significant because it signifies a change in the predominant mechanisms governing the conduction transport within the semiconductor device; although, for the unirradiated samples, the conduction mechanism at 307 K is primarily dictated by the diffusion component. However, as the irradiation fluence increases, the non-ideality factor *n* also increases, and this leads to a shift in the conduction mechanism. The device begins to rely more heavily on the generation-recombination component, which involves the creation and recombination of electron–hole pairs, in addition to diffusion. Remarkably, this observed behavior mirrors the changes induced by irradiation in the series resistance (R_s), as explained earlier. Both the increase in 'n' and the elevation in R_s suggest that irradiation modifies the underlying physics of the semiconductor, affecting the relative contributions of diffusion and generation-recombination currents to the conduction mechanism. This nuanced understanding of the interplay between *n* and R_s is invaluable in modeling and optimizing semiconductor devices under radiation conditions and is highly relevant in fields where radiation tolerance and performance are critical.

Table 1 serves as a concise and informative representation of irradiation's impact on the ideality factor *n* based on observations in Domain II. Interestingly, the behavior of *n* in response to irradiation closely mirrors the trends observed in Domain I. In both domains, *n* consistently exceeds the conventional value of 2, prompting intriguing inquiries into the fundamental physics governing the emitter-base junction during irradiation. The observation that *n* surpasses 2 suggests the possible influence of additional current components beyond those conventionally associated with the ideality factor. This discrepancy implies the existence of further factors or mechanisms within the semiconductor device when ex- posed to irradiation. As a result, there is a compelling need for comprehensive investigation and analysis to uncover the precise nature of these

supplementary components and their impact on the overall junction current. This deeper understanding is crucial for enhancing models and enhancing the reliability and performance of semiconductor devices when operating in radiation-intensive environments.

Table 1. The impact of irradiation on the non-ideality factor (n) of the silicon NPN E-B junction asa function of 1 MeV proton irradiation fluences at 307 K in Domain II, where "NI" designates the condition of no irradiation.

Φ ($p.cm^{-2}$)	NI	5.3×108	5.3×1010	5×1011	5×1012	5×1013
N(307K)	2.1	2.5	2.9	3.4	3.1	3.9

Figure 6 displays the reverse bias I–V characteristics of a silicon (NPN) emitter-base junction at 307 K, taking into account the impact of proton irradiation. The label 'NI' denotes the condition of an unirradiated sample. The data presented in this figure demonstrate that, for voltages below 7.2 V, the current flowing through the silicon (NPN) emitter-base junction remains practically negligible. However, as the applied voltage exceeds this critical threshold, a remarkable phenomenon unfolds; the current begins to exhibit exponential growth. This remarkable behavior can be attributed to the substantial increase in the electric field intensity within the junction. This intensification of the electric field is sufficient to create electron–hole pairs within the semiconductor material, which, in turn, sets the stage for what is known as the avalanche phenomenon. The avalanche effect occurs when the electric field is strong enough to trigger a chain reaction of electron–hole pair generation. This process significantly amplifies the current, leading to the exponential growth observed in the graph. It is important to note that, as the level of irradiation fluence increases, there is a discernible elevation in the knee voltage, which is the point at which the current starts to exhibit this exponential growth. For instance, in unirradiated samples, the knee voltage measures 7.2 V. However, as the irradiation fluence intensifies to 10^{13} p/cm^2, the knee voltage noticeably increases to 8.3 V.

Moreover, the observation of higher breakdown voltage in the reverse current at higher radiation levels is indeed an important aspect that warrants clarification. This phenomenon can be attributed to the influence of irradiation on the electrical properties of the semiconductor material. As radiation increases, defectsand traps are introduced into the material, affecting its ability to maintain a low reverse current. This correlation between irradiation level and the knee voltage underscores the significant impact of irradiation on the electrical behavior of the junction, providing critical insights for understanding the radiation tolerance and performance that are paramount of the device.

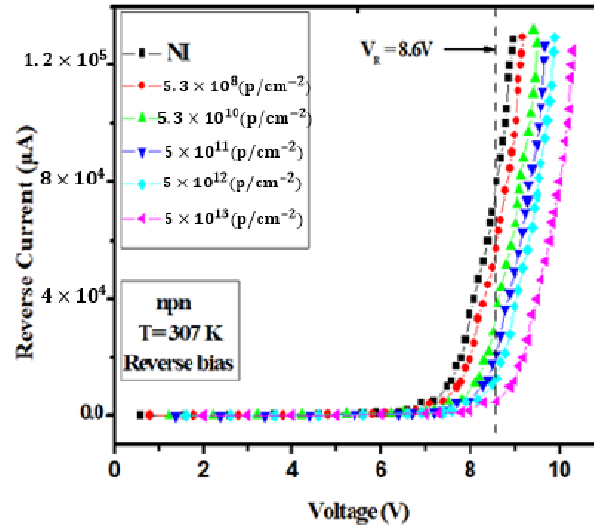

Figure 6. The reverse bias I–V characteristics of silicon (NPN) emitter-base junction at 307 K, considering the influence of proton irradiation. "NI" designates the condition of an unirradiated sample.

Figure 7 depicts the impact of 1 MeV proton irradiation on current at constant reverse and forward polarizations at 307 K in a silicon NPN EBJ. It is evident that the current exhibits a diminishing trend as irradiation fluences increase, a behavior that approximates a linear decline. Consequently, we have defined experimental linear degradation factors, following the same methodology as for R_s and I_s. Specifically, we have determined linear degradation factors of (6.61 ± 0.98) $\times 10^{-16}$ cm^2 per proton for forward bias and (1.53± 0.23) $\times 10^{-15}$ cm^2 per proton for reverse bias. It is noteworthy that the degradation of reverse current is more pronounced compared to that of forward current for both polarization states. This observed degradation in both forward and reverse currents can be attributed to the capture of charge carriers by defects introduced into the forbidden band, implying a substantial doping compensation effect induced by irradiation.

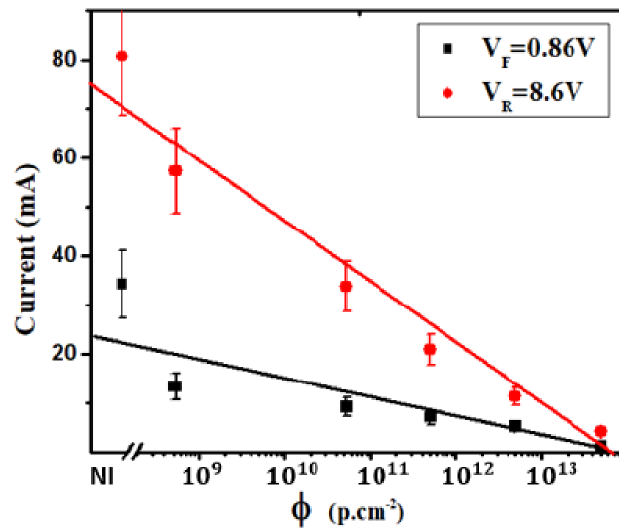

Figure 7. The impact of 1 MeV proton irradiation on the current for constant reverse and forwardpolarizations at 307 K in silicon NPN emitter-base junction.

It is well-established that the introduction of defects increases as a function of irradiation fluences. These defects manifest at various energy levels within the semiconductor band gap, often linked to different structural defects that can range from specific to complex in nature. These energy levels are established through an experimental technique, including deep-level transient spectroscopy (DLTS). As demonstrated by [16], irradiation in silicon introduces two distinct defects situated at energy levels of 0.19 eV and 0.35 eV, which are attributed to complexes associated with oxygen. Additionally, other defects have been reported, including donor defects at energy levels of 0.24 eV and 0.35 eV, which are ascribed to copper, and acceptor defects at energy levels of 0.49 eV and 0.54 eV, which are linked to gold [31]. Furthermore, it was reported by Watkins et al. [32,33] that this irradiation effect leads to the creation of two distinct defects within the silicon material. The first defect, denoted as the A center, is situated at an energy level of 0.17 eV. This A center is attributed to complexes formed by silicon vacancies and oxygen atoms. The second defect, known as the E center, is located at an energy level of 0.4 eV. It corresponds to complexes formed by silicon vacancies and a weak donor, particularly phosphorus (P).At the temperature of 307 K, the dominant conduction mechanism within Domain I is diffusion.

However, with increasing irradiation fluences, the density of generation centers also increases, as discussed earlier. Consequently, conduction becomes increasingly reliant on the generation-recombination component, thereby corroborating the observed rise in the non-ideality factor (n). This observed behavior aligns consistently with the results obtained for R_s and I_s, as per the irradiation dependencies discussed earlier. The factors k_R and k_I provide additional insights, suggesting that the defects introduced into the silicon junction, which primarily contribute to the increase in I_s, do not entirely account for the rise in R_s. Furthermore, the values obtained for n in Domain II suggest that forward current modeling should encompass the consideration of additional components such as tunneling effects, surface diffusion effects, and surface generation-recombination effects. This implies that the surface effects may be attributed to suboptimal passivation of the silicon junctions. For both polarization states, the recurring trend of decreasing current with increasing irradiation fluences is noteworthy. Consequently, we can confidently assert that the principal effect of irradiation is to compensate for doping rather than reinforce it. In other words, the introduction of donor defects is dominated by the introduction of acceptor centers.

4. CONCLUSIONS

In conclusion, our study investigated the irradiation effects on silicon (NPN) emitter- base junctions at 307 K. We focused on various electrical characteristics, including series resistance (R_s), saturation current (I_s), and the non-ideality factor (n), under both forward and reverse polarization. Our findings revealed that irradiation induced significant changes in these parameters, with R_s and I_s showing linear dependencies on irradiation fluence. Nevertheless, n exhibited a more pronounced increase than R_s, indicating that defects introduced by irradiation did not contribute equally to both. Moreover, our results demonstrated that irradiation compensated for doping rather than reinforcing it, suggesting a dominant role for acceptor centers. These insights contribute to our understanding of semiconductor behavior under irradiation, with potential implications for the design and reliability of electronic devices in 1 MeV proton-irradiation environments.

REFERENCES

1. Hassan, A.; Savaria, Y.; Sawan, M. Electronics and Packaging Intended for Emerging Harsh Environment Applications: A Review. *IEEE Trans. Very Large Scale Integr. VLSI Syst.* **2018**, *26*, 2085–2098. [CrossRef]

2. Burr, G.W.; Kurdi, B.N.; Scott, J.C.; Lam, C.H.; Gopalakrishnan, K.; Shenoy, R.S. Overview of candidate device technologies for storage-class memory. *IBM J. Res. Dev.* **2008**, *52*, 449–464. [CrossRef]
3. Liu, G.; Tuttle, B.R.; Dhar, S. Silicon carbide: A unique platform for metal-oxide-semiconductor physics. *Appl. Phys. Rev.* **2015**, *2*. [CrossRef]
4. Park, H.; Boyer, K.; Clawson, C.; Eiden, G.; Tang, A.; Yamaguchi, T.; Sachitano, J. High-speed polysilicon emitter—Base bipolar transistor. *IEEE Electron Device Lett.* **1986**, *7*, 658–660. [CrossRef]
5. Neugroschel, A.; Sah, C.-T.; Carroll, M. Degradation of bipolar transistor current gain by hot holes during reverse emitter-base bias stress. *IEEE Trans. Electron Devices* **1996**, *43*, 1286–1290. [CrossRef]
6. Gopiraj, A.; Billimagga, R.S.; Ramasubramanian, V. Performance characteristics and commissioning of MOSFET as an in-vivo dosimeter for high energy photon external beam radiation therapy. *Rep. Pract. Oncol. Radiother.* **2008**, *13*, 114–125. [CrossRef]
7. Meguellati, M.; Djeffal, F. New Dual-Dielectric Gate All Around (DDGAA) RADFET dosimeter design to improve the radiation sensitivity. *Nucl. Instrum. Methods Phys. Res. Sect. A Accel. Spectrometers Detect. Assoc. Equip.* **2012**, *683*, 24–28. [CrossRef]
8. Tamersit, K.; Djeffal, F. A novel graphene field-effect transistor for radiation sensing application with improved sensitivity: Proposal and analysis. *Nucl. Instrum. Methods Phys. Res. Sect. A Accel. Spectrometers Detect. Assoc. Equip.* **2018**, *901*, 32–39. [CrossRef]
9. Holmes-Siedle, A.; Adams, L. RADFET: A review of the use of metal-oxide-silicon devices as integrating dosimeters. *Int. J. Radiat. Appl. Instrum. Part C Radiat. Phys. Chem.* **1986**, *28*, 235–244. [CrossRef]
10. Ahmed, S.N. *Physics and Engineering of Radiation Detection*; Academic Press: Cambridge, MA, USA, 2015; ISBN 9780128013632.
11. Dale, C.; Marshall, P.; Burke, E.; Summers, G.; Wolicki, E. High energy electron induced displacement damage in silicon. *IEEE Trans. Nucl. Sci.* **1988**, *35*, 1208–1214. [CrossRef]
12. Leroy, C.; Rancoita, P.-G. Particle interaction and displacement damage in silicon devices operated in radiation environments. *Rep. Prog. Phys.* **2007**, *70*, 493–625. [CrossRef]
13. Srour, J.; Marshall, C.; Marshall, P. Review of displacement damage effects in silicon devices. *IEEE Trans. Nucl. Sci.* **2003**, *50*, 653–670. [CrossRef]
14. Summers, G.P.; Burke, E.A.; Dale, C.J.; Wolicki, E.A.; Marshall, P.W.; Gehlhausen, M.A. Correlation of Particle-Induced Displace- ment Damage in Silicon. *IEEE Trans. Nucl. Sci.* **1987**, *34*, 1133–1139. [CrossRef]
15. Schrimpf, R.D.; Fleetwood, D.M.; Normand, E.; Baumann, R.C.; McMORROW, D.; Melinger, J.S.; Knudson, A.R.; Fouillat, P.; Pouget, V.; Lewis, D.; et al. *Radiation Effects and Soft Errors in Integrated Circuits and Electronic Devices*; World Scientific: Singapore, 2004; ISBN 9789810218621.
16. Ohyama, H.; Vanhellemont, J.; Simoen, E.; Claeys, C.; Takami, Y.; Hayama, K.; Yoshimoto, K.; Sunaga, H.; Kobayashi, K. Substrate effects on the degradation of irradiated Si diodes. In Proceedings of the Third European Conference on Radiation and Its Effects on Components and Systems, Arcachon, France, 18–22 September 1995; pp. 72–79.
17. Hefner, A.R.; Blackburn, D.L.; Galloway, K.F. The Effect of Neutrons on the Characteristics of the Insulated Gate Bipolar Transistor (IGBT). *IEEE Trans. Nucl. Sci.* **1986**, *33*, 1428–1434. [CrossRef]
18. Omotoso, E.; Paradzah, A.; Diale, M.M.; Coelho, S.M.M. The influence of high energy electron irradiation on the Schottky barrier height and the Richardson constant of Ni/4H-SiC Schottky diodes. *Mater. Sci. Semicond. Process.* **2015**, *39*, 112–118. [CrossRef]
19. Pearton, S.J.; Ren, F.; Patrick, E.; Law, M.E.; Polyakov, A.Y. Review—Ionizing Radiation

Damage Effects on GaN Devices. *ECS J. Solid State Sci. Technol.* **2015**, *5*, Q35–Q60. [CrossRef]

20. Pearton, S.J.; Hwang, Y.-S.; Ren, F. Radiation Effects in GaN-Based High Electron Mobility Transistors. *JOM* **2015**, *67*, 1601–1611. [CrossRef]
21. Schwarz, C.; Yadav, A.; Shatkhin, M.; Flitsiyan, E.; Chernyak, L.; Kasiyan, V.; Liu, L.; Xi, Y.Y.; Ren, F.; Pearton, S.J.; et al. Gamma irradiation impact on electronic carrier transport in AlGaN/GaN high electron mobility transistors. *Appl. Phys. Lett.* **2013**, *102*, 062102. [CrossRef]
22. Elghazi, H.; Jorio, A.; Zorkani, I. Analysis of temperature and 1MeV proton irradiation effects on the light emission in bulk silicon (npn) emitter-base bipolar junctions. *Opt. Commun.* **2007**, *280*, 278–284. [CrossRef]
23. El Ghazi, H.; Jorio, A.; Zorkani, I. Analysis of silicon light emission under breakdown condition using an indirect intraband model. *Opt. Commun.* **2008**, *281*, 3320–3323. [CrossRef]
24. EL Ghazi, H.; Jorio, A.; Zorkani, I.; Ouazzani-Jamil, M. Optical characterization of InGaN/AlGaN/GaN diode grown on silicon carbide. *Opt. Commun.* **2008**, *281*, 3314–3319. [CrossRef]
25. N2219A STMicroelectronics | Mouser', Mouser Electronics. Available online: https://eu.mouser.com/ProductDetail/511-2N2219A (accessed on 11 October 2023).
26. Sah, C.T.; Lindholm, F.A.; Neugroschel, A.; Electrical Engineering Dept. *NASA Conference Publication. Volume No. 2020–2021*; Scientific and Technical Information Office, National Aeronautics and Space Administration: Washington, DC, USA, 1977.
27. Burke, E.A. Energy Dependence of Proton-Induced Displacement Damage in Silicon. *IEEE Trans. Nucl. Sci.* **1986**, *33*, 1276–1281.[CrossRef]
28. Jia, Y.; Zhang, Z.; Bi, D.; Hu, Z.; Zou, S. Effect of Total Dose Irradiation on Parasitic BJT in 130 nm PDSOI MOSFETs. *Micromachines* **2023**, *14*, 1679. [CrossRef]
29. Jeon, D.-Y.; Park, S.J.; Mouis, M.; Barraud, S.; Kim, G.-T.; Ghibaudo, G. Impact of series resistance on the operation of junctionless transistors. *Solid-State Electron.* **2017**, *129*, 103–107. [CrossRef]
30. Sun, Y.; Wang, T.; Liu, Z.; Xu, J. Investigation of irradiation effects and model parameter extraction for VDMOS field effect transistor exposed to gamma rays. *Radiat. Phys. Chem.* **2021**, *185*, 109478. [CrossRef]
31. Baru, V.G.; VOL'KENŠTEJN, F. *Effet de L'irradiation sur les Propriétés des Semi-Conducteurs*; Mir Publisher: Moscow, Russia, 1982.
32. Watkins, G.D. *Radiation Damage in Semiconductors*; Dunod: Paris, France, 1965.
33. Watkins, G.D. Optical properties of group-V atom-vacancy pairs in silicon. *Radiat. Eff. Defects Solids* **1989**, *111*, 487–500. [CrossRef]